
Research Article: Methods/New Tools | Novel Tools and Methods

Limited sensitivity of hippocampal synaptic function or network oscillations to unmodulated kilohertz electric fields

<https://doi.org/10.1523/ENEURO.0368-20.2020>

Cite as: eNeuro 2020; 10.1523/ENEURO.0368-20.2020

Received: 25 August 2020

Revised: 3 November 2020

Accepted: 5 November 2020

This Early Release article has been peer-reviewed and accepted, but has not been through the composition and copyediting processes. The final version may differ slightly in style or formatting and will contain links to any extended data.

Alerts: Sign up at www.eneuro.org/alerts to receive customized email alerts when the fully formatted version of this article is published.

Copyright © 2020 Esmailpour et al.

This is an open-access article distributed under the terms of the Creative Commons Attribution 4.0 International license, which permits unrestricted use, distribution and reproduction in any medium provided that the original work is properly attributed.

1 **Limited sensitivity of hippocampal synaptic function or network oscillations to**
2 **unmodulated kilohertz electric fields**

3

4 Zeinab Esmailpour¹, Mark Jackson¹, Greg Kronberg¹, Tianhe Zhang², Rosana Esteller², Brad
5 Hershey², Marom Bikson¹

6

7 ¹ Neural Engineering Laboratory, Department of Biomedical Engineering, The City College of
8 the City University of New York, City College Center for Discovery and Innovation New
9 York NY USA.

10 ² Boston Scientific Neuromodulation, Boston, MA, USA.

11

12 **Abstract:**

13 Understanding the cellular mechanisms of kHz electrical stimulation is of broad interest in
14 neuromodulation including forms of transcranial electrical stimulation (tES), interferential
15 stimulation, and high-rate spinal cord stimulation (SCS). Yet, the well-established low-pass
16 filtering by neuronal membranes suggests minimal neuronal polarization in response to charge-
17 balanced kHz stimulation. The hippocampal brain slice model is among the most studied
18 systems in neuroscience and exhaustively characterized in screening the effects of electrical
19 stimulation. High-frequency electric fields of varied amplitudes (1-150 V/m), waveforms
20 (sinusoidal, symmetrical pulse, asymmetrical pulse) and frequencies (1 and 10 kHz) were tested.
21 Changes in single or paired-pulse field excitatory post-synaptic potentials (fEPSP) in CA1 were
22 measured in response to radial- and tangential-directed electric fields, with brief (30 s) or long
23 (30 min) application times. The effects of kHz stimulation on ongoing endogenous network

24 activity were tested in carbachol-induced gamma oscillation of CA3a and CA3c. Across 23
25 conditions evaluated, no significant changes in fEPSP were resolved, while responses were
26 detected for within-slice control DC fields. 1 kHz sinusoidal and pulse stimulation (≥ 60 V/m), but
27 not 10 kHz induced changes in oscillating neuronal network. We thus report no responses to
28 low-amplitude 1 kHz or any 10 kHz fields, suggesting that any brain sensitivity to these fields is
29 via yet to be-determined mechanism(s) of action which were not identified in our experimental
30 preparation.

31 **Key words:** High-frequency stimulation, kilohertz electrical stimulation, neuronal excitability,
32 brain stimulation, gamma oscillation

33

34

35 **SIGNIFICANCE STATEMENT:**

36 There a large mismatch between enthusiasm for clinical treatments using kHz frequency
37 electrical stimulation and the understanding of kHz mechanisms of action. Indeed, the well-
38 established low-pass properties of cell membranes should attenuate any response to kHz
39 stimulation. This study presents the largest and broadest characterization of the cellular effects
40 of kHz stimulation using the most established animal model to detect CNS sensitivity to electric
41 fields: Our work systematically evaluated sensitivity of hippocampal synaptic function and
42 oscillatory network activity in response to kHz. Only at low kHz (1 kHz but not 10 kHz) with high
43 intensity and during oscillations responses were detected. This systematic and largely negative
44 experimental series suggest kHz neuromodulation operates via yet to be determined
45 mechanisms.

46

49 Introduction

50

51 Electric fields at low frequencies (<100 Hz) are highly effective in changing firing rate
52 and timing of neuronal population (Fröhlich and McCormick, 2010; McIntyre et al., 2004),
53 including at very low (~ 1 V/m) intensities (Reato et al., 2010). However, as the frequency of
54 electric field oscillations increases beyond a few hundred hertz, sensitivity to stimulation and
55 brain responses diminishes (Deans et al., 2007). On the one hand, this is readily attributable to
56 the low-pass filtering characteristics of cell membranes (Bikson et al., 2004; Deans et al., 2007;
57 McIntyre and Grill, 1999; Ranck, 1975). Emerging neuromodulation techniques specifically
58 using kHz frequency stimulation have been developed, in some cases with marked clinical
59 efficacy. This includes transcranial Alternating Current Stimulation (tACS) with sinusoidal kHz
60 waveforms (Chaieb et al., 2011), transcranial Random Noise Stimulation (tRNS) (Antal and
61 Paulus, 2013; Laczó et al., 2014; Terney et al., 2008), kHz Spinal Cord Stimulation (SCS)
62 (Bradley and Redwood City, 2017; Kapural et al., 2015), and recently, kHz Deep Brain
63 Stimulation (DBS) (Harmsen et al., 2019; Khadka et al., 2020). Approaches using interferential
64 or intersectional short pulse stimulation (Esmailpour et al., 2020; Grossman et al., 2017;
65 Voroslakos and Takeuchi, 2018) are a special case underpinned by an assumption of sensitivity
66 to amplitude modulated kHz field, but no responses to unmodulated kHz stimulation.

67 Across this proliferation of techniques and application of kHz neuromodulation, the
68 cellular mechanisms of kHz electrical stimulation remain unclear (Dmochowski and Bikson,
69 2017; Pelot et al., 2017). While, at very high stimulation intensities, kHz stimulation may
70 produce supra-physiological changes (e.g. conduction block (Crosby et al., 2017; Zhang et al.,
71 2006), electroporation (Dowden et al., 2010)), for existing clinical applications these intensities
72 are not expected at target tissue. Given that the response of neurons to kHz electrical
73 stimulation is attenuated, the possibility of sub-threshold stimulation of baseline neuronal activity

74 (where ongoing neuronal activity is modulated; (Bikson and Rahman, 2013)) is considered
75 alongside supra-threshold stimulation (de novo generation of action potentials / pacing).

76 Our goal was to systematically evaluate the sensitivity of hippocampal synaptic function
77 and oscillatory network activity to kilohertz frequency extracellular electrical stimulation. For
78 assessing the sub and supra-threshold effects of electric stimulation on brain excitability, the
79 application of uniform electric fields across the rodent slice preparation is among the longest-
80 standing and most exhaustively studied animal models (Bikson et al., 2004; Jackson et al.,
81 2016; Jefferys, 1981). fEPSPs, including pair-pulse responses, are sensitive to modulation by
82 electric fields through changes in axonal excitability (Kabakov et al., 2012; Rahman et al.,
83 2017), synaptic activity (Rahman et al., 2013), dendritic activity (Bikson et al., 2004; Kronberg et
84 al., 2017), and somatic activity (Fröhlich and McCormick, 2010; Radman et al., 2009), while
85 generally providing a global index for excitatory and inhibitory synaptic efficacy (Jefferys, 1981),
86 information processing (Gluckman et al., 1996; Lafon et al., 2017; Radman et al., 2007), and
87 plasticity (Fritsch et al., 2010; Kronberg et al., 2017; Ranieri et al., 2012). Neuronal network
88 oscillations, including those in the gamma frequency band, are highly sensitive to electric fields
89 through well-characterized mechanisms of amplification (Deans et al., 2007; Fröhlich and
90 McCormick, 2010; Reato et al., 2010).

91 Here, we use fEPSP and oscillations to test the effect of 1- and 10-kHz electrical
92 stimulation using sinusoidal symmetric and asymmetric pulse waveforms. We used direct
93 current (DC) electrical stimulation as a within-slice control to confirm the sensitivity to low-
94 frequency stimulation. Our data suggest the presence of diminished neuronal sensitivity in
95 response to kHz stimulation consistent with the dramatic low-pass filtering property of the
96 neuronal membrane. Oscillatory networks (e.g. gamma oscillation) are more sensitive to
97 electrical stimulation but only to 1 kHz stimulation at ≥ 60 V/m intensity. Thus, consistent with
98 results using sub-kHz electric fields, the structure of ongoing network oscillations would

99 determine maximal sensitivity and effects of stimulation (Reato et al., 2013). If the brain is
100 sensitive to high-kHz frequencies (i.e. 10 kHz) or lower-amplitude stimulation, it may be via
101 mechanisms yet to be identified in the brain slice preparation (e.g. peculiarly sensitive neuronal
102 elements, non-neuronal elements such as neuroglia, vascular response, heating), effects
103 peculiar to non-uniform fields, and/or effects with a gradual (e.g. hours) onset.

104

105 **Methods**

106

107 All animal experiments were carried out in accordance with guidelines and protocols
108 approved by the Institutional Animal Care and Use Committee at The City Collage of New York,
109 CUNY.

110 *Hippocampal slice preparation:* Hippocampal brain slices were prepared from male
111 Wistar rats aged 3–5 weeks old, which were deeply anaesthetized with ketamine (7.4 mg kg⁻¹)
112 and xylazine (0.7 mg kg⁻¹) applied I.P. and sacrificed by cervical dislocation. The brain was
113 quickly removed and immersed in chilled (2–6 °C) dissecting solution containing (in mM) 110
114 choline chloride, 3.2 KCl, 1.25 NaH₂PO₄, 26 NaHCO₃, 0.5 CaCl₂, 7 MgCl₂, 2 sodium
115 ascorbate, 3 sodium pyruvate, 10 D-glucose. Transverse hippocampal slices (400 μm thick)
116 were cut using a vibrating microtome (Campden Instruments, Leicester, England) and
117 transferred to a recovery chamber for 30 minutes at 34 °C with a modified artificial cerebrospinal
118 fluid (ACSF) containing (in mM) 124 NaCl, 3.2 KCl, 1.25 NaH₂PO₄, 26 NaHCO₃, 2.5 CaCl₂, 1.3
119 MgCl₂, 2 sodium ascorbate, 3 sodium pyruvate, and 25 D-glucose. Slices were then
120 transferred to a holding chamber for at least 30 minutes (or until needed) at 30 °C with ACSF
121 containing (in mM) 124 NaCl, 3.2 KCl, 1.25 NaH₂PO₄, 26 NaHCO₃, 2.5 CaCl₂, 1.3 MgCl₂, and
122 25 D-glucose. For fEPSP experimental recordings, slices were then transferred to a fluid–gas
123 interface recording chamber (Hass top model, Harvard Apparatus, Holliston MA, USA) perfused

124 with warmed ACSF (30.0 ± 0.1 °C) at 1.0 ml min^{-1} . For gamma oscillation experiments, slices
125 were transferred to a fluid–gas interface recording at 34 °C. All solutions were saturated with a
126 gas mixture of 95% O₂–5% CO₂. Gamma oscillations were induced by perfusing the slices with
127 ACSF containing 20 μM carbachol (carbamoylcholine chloride). All reagents were purchased
128 from Sigma Aldrich (St. Louis MO, USA).

129 **fEPSP recording (acute and long-term):** Recordings started 30 minutes after transfer
130 to the recording chamber. fEPSPs were evoked in the Schaffer collateral pathway using a
131 platinum–iridium bipolar stimulating electrode placed in stratum radiatum of CA1 approximately
132 300 μm from stratum pyramidale. Recording electrodes made from glass micropipettes
133 (Aluminosilicate glass with 1.5 mm outer diameter, 1.0 mm inner diameter) pulled by a Sutter
134 Instruments P-97 (Novato CA, USA) and filled with ACSF (resistance 0.5–2 M Ω) were placed in
135 stratum radiatum of CA1, approximately 400 μm from the stimulating electrode and within 100
136 μm from stratum pyramidale (Figure 1). fEPSPs were quantified by the average initial slope,
137 taken during the first 0.5 ms after the onset of the fEPSP. Stimulus intensity was set to evoke
138 fEPSPs with 35–50% of the maximum slope, which was determined at the onset of recording.
139 For paired pulse facilitation (PPF) experiments, two fEPSPs were evoked at a 50 ms interval
140 (Korte et al., 1995; Kronberg et al., 2017; Lessmann and Heumann, 1998). PPF was quantified
141 as the ratio of the second to the first fEPSP slope in each condition.

142 For acute experiments, fEPSPs were evoked every 30 s, alternating between control
143 and kHz (or DCS) conditions. Waveforms were applied for 1 s and fEPSPs were evoked
144 midway (0.5 s, mid-field, MF) through the stimulation (Figure 1). Where indicated, fEPSPs were
145 also evoked 0.1 ms after the extracellular field was turned off (post-field, PF). For control
146 conditions, fEPSPs were evoked alone (no kHz stimulation). Within a given slice, a single kHz
147 waveform was tested at multiple intensities in a randomized order ranging from 1–80 V/m (1, 5,
148 10, 20, 40, 60, and 80 V/m) with each intensity repeated 3 to 15 times per slice. fEPSP slopes

149 during each kHz epoch were normalized to the average of the control fEPSP slopes
150 immediately preceding and following it. Normalized fEPSP slopes were then averaged across
151 the repeats for each intensity, producing one n per slice per waveform.

152 For long-term experiments, fEPSPs were evoked every 30 s and fEPSP slope was
153 monitored online. After at least 30 minutes of stable baseline fEPSP recordings, 1 and 10 kHz
154 waveforms were applied parallel to the somato-dendritic axis (radial) at 80 V/m for 30 minutes.
155 fEPSPs were continuously evoked every 30 s throughout the kHz and for 60 minutes after kHz
156 ended. To determine stability prior to stimulation, a least squares linear fit was applied to the
157 baseline fEPSP slopes. The slope of the linear fit ($\text{mVms}^{-1}\text{min}^{-1}$) was required to be less than
158 0.33 % of the mean baseline fEPSP slopes (i.e. less than 20% drift expected over 60 minutes).
159 For the control condition, the same stability criteria were used, but no stimulation was applied.
160 To quantify long-term effects, fEPSP slopes were normalized to the mean of the 20 minutes
161 immediately preceding high frequency stimulation. Sampling frequency was reduced to 10 kHz
162 during long-term experiments in both 1 and 10 kHz stimulation due to technical limitations. The
163 responses were compared between sham and control condition in three different times
164 (immediately, 30 minutes and 60 minutes after termination of stimulation).

165 *Data analysis:* All data are reported as the mean \pm standard error of the mean (SEM).
166 Reported n values represent the number of slices used in each condition. Statistical analysis
167 was performed using unpaired, one sample t-test for positive and negative DC control
168 stimulation, after checking for normality in each group (Lilliefors test for normality, $p > 0.05$ in all
169 cases) and one-way repeated measure ANOVA for different intensities used in kHz waveforms.
170 Bonferroni correction was used for multiple comparison correction. All the analysis was
171 performed in R (RStudio, Inc., Boston, MA).

172

173 Bayesian inference:

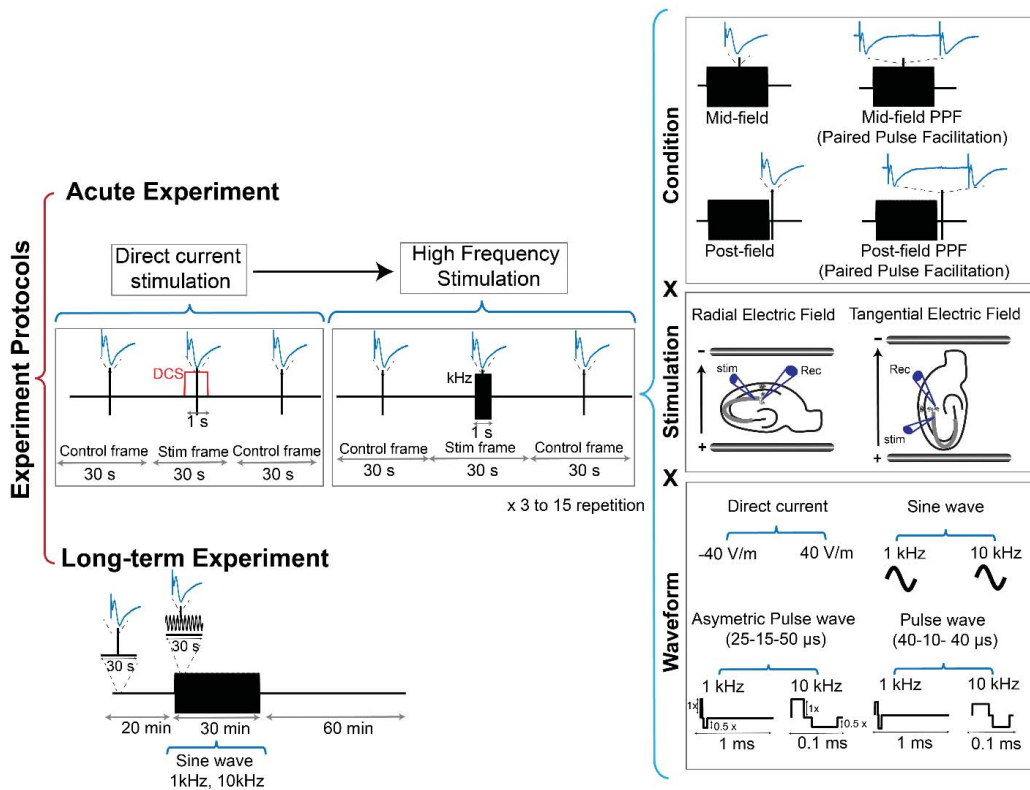
174 Difference across highest electric field intensity and baseline were analyzed using the
175 Bayesian paired samples T-test as implemented in JASP v0.13.1.0 using default effect size
176 prior (Cauchy 0.707) (Keysers et al., 2020). Results are reported using two tailed Bayes factor
177 BF_{+0} that represents $p(H_+ | 80 \text{ v/m} \neq \text{baseline}) / p(H_0 | 80 \text{ v/m} = \text{baseline})$. Effect size estimates
178 are reported as median posterior Cohen's d with 95% credibility interval using a two-tailed H_1 in
179 order not to bias estimates in the expected direction. Bayesian ANOVAs were conducted using
180 JASP with default priors, and effects are reported as Bayes factor for the inclusion of a
181 particular effect, calculated as the ratio between the likelihood of the data given the model with
182 vs the next simpler model without that effect.

183 *Electrical field stimulation:* kHz and DCS extracellular electric fields were applied to
184 slices via two parallel Ag–AgCl wires (1 mm diameter, 12 mm length, 10 mm apart) placed in
185 the recording chamber on opposite sides of the brain slice with the recording site approximately
186 equidistant from each wire. Slices were oriented so that the resulting electric field was either
187 parallel (radial stimulation) or perpendicular (tangential stimulation) to the somato-dendritic axis
188 of CA1 pyramidal neurons (Figure 1). In CA3 experiments, slices were oriented so that the
189 resulting electric field was parallel to the main somato-dendritic axis of CA3a pyramidal neurons
190 (perpendicular to pyramidal cell layer, figure 1 A.1). Field wires were connected to a custom
191 high band-width voltage-controlled isolated current source. Before each recording, the applied
192 current intensity was calibrated by measuring the electric field (voltage difference between two
193 recording electrodes separated by 0.8 mm in the slice) in response to a 10 μA DC test pulse.
194 This characterized the linear relationship between electric field magnitude and applied current,
195 which was then used to determine the current intensity required for a desired electric field. Data
196 acquisition and stimulation waveforms were controlled by Power1401-625 kHz hardware and
197 Signal software Version 6.0 (Cambridge Electronic Design (CED), Cambridge, UK). Voltage

198 signals were amplified (10x), analog low pass filtered (20 kHz; Model 3000 differential amplifier,
199 A-M systems, Carlsborg WA, USA) and digitized (200 kHz, Power1401-625 kHz and Signal,
200 CED, Cambridge, UK). Prior to analyzing the fEPSP slope, all signals were digitally low pass
201 filtered with Signal 6.0 (FIR filter, 2047 coefficients, 250 Hz transition gap, 1,099 -3 dB) or
202 MATLAB to remove stimulation artifact (700 Hz cut-off for 1 kHz stimulation and 1 kHz cut-off for
203 10 kHz stimulation).

204 kHz was applied at 1 and 10 kHz using the following kHz waveforms (leading polarity
205 pulse width - interphase interval - opposite polarity pulse width): sinusoid, pulse (40-10-40 μ s for
206 1 kHz and 10 kHz), and an asymmetric pulse waveform with the shorter duration pulse at 2x the
207 amplitude of the longer duration pulse (25-15-50 μ s for 10 kHz) (Figure 1). Reported magnitude
208 for the asymmetric pulse waveform is the electric field during the leading (shorter) pulse. For
209 each slice, DCS at 40 V/m was applied with alternating polarity before kHz waveforms as a
210 basis for comparing effect sizes. Here positive, radial +DCS refers to uniform DC electric fields
211 that are parallel to the somato-dendritic axis of CA1 pyramidal neurons, with the positive
212 terminal closer to the apical dendrites (as opposed to basal dendrites). Positive, tangential DCS
213 refers to uniform DC electric fields that are parallel to Schaffer collaterals in CA1 with DCS
214 current flow in the same direction as orthodromic action potential propagation (Figure 1). Unless
215 otherwise stated, the electric field reported throughout the manuscript is the peak electric field
216 for each waveform.

217



218

219 **Figure 1:** Experimental design of hippocampal slice recordings. *Acute experiments:* Direct current stimulation as
 220 within-slice control condition before high frequency stimulation paradigm. fEPSP was evoked and recorded in 4
 221 different conditions: Mid-field, Mid-field PPF, Post-field and Post-field PPF. Bipolar stimulation and glass recording
 222 electrodes depicted in CA1 stratum radiatum along with a pyramidal neuron and Schaffer collateral (gray).
 223 *Stimulation:* field wires were placed on opposite sides across the slice and connected to a current source. In radial
 224 configuration electric fields were applied parallel to the CA1 pyramidal somato-dendritic axis and in tangential
 225 configuration, electric fields were applied perpendicular to the CA1 pyramidal somato-dendritic axis. *Waveform:* Direct
 226 current and various electric field waveforms for kHz stimulation. The duration of each waveform component is given
 227 in μ s for 1 kHz and 10 kHz stimulation. Alternating control and kHz (or direct current) epochs were repeated every 30
 228 s. Raw data were low pass filtered to obtain fEPSPs for analysis. fEPSP obtained during kHz/DCS (mid-field) or 0.1
 229 ms after kHz/DCS (post-field) were normalized to the average of preceding and following fEPSP. Long-term
 230 Experiment: fEPSP was evoked every 30 seconds. Stimulation was applied for 30 min after a 20 min stable baseline.
 231 Field EPSP recording was continued 1 hour after the end of stimulation.

232

233 **Extracellular recordings (Gamma oscillation):** Recordings of extracellular field
234 potentials in the pyramidal layer of CA3a and CA3c region of hippocampus were obtained using
235 glass micropipettes (15 M Ω pulled on a P-97, Sutter instruments) field with ACSF. Data
236 acquisition and electrical stimulation were controlled by Power1401-625 kHz hardware and
237 Signal software Version 6.0 (Cambridge Electronic Design (CED), Cambridge, UK). Voltage
238 signals were amplified (10x), analog low pass filtered (20 kHz; Model 3000 differential amplifier,
239 A-M systems, Carlsberg WA, USA) and digitized (20 kHz, Power1401-625 kHz and Signal,
240 CED, Cambridge, UK). To reduce noise and stimulation artifacts, the voltage recordings were
241 always performed relative to an iso-potential electrode placed in bath (Figure 6, A.1). Field
242 recordings overcome potential limitations of intracellular recording during kHz field such as
243 current collection by the capacitive-walled microelectrode leading to artifactual intracellular
244 stimulation (FallahRad et al., 2019) or possible amplifier distortion (Lesperance et al., 2018).

245 **Power analysis and statistics:** Signals were recorded in frames of 5 s (1.5 s before and
246 1.5 s after stimulation) and stimulation was applied for 2 s. Stimulation artifacts were minimized
247 by subtracting the voltage in an iso-potential reference electrode from the recording electrode in
248 the slice (Figure 6). Spectrograms were computed (200 ms hamming window, 90% overlap) on
249 individual 5 s frames and averaged over 100 frames for each stimulation condition (i.e.
250 frequency, waveform and amplitude). Normalized power was measured as a power ratio
251 normalized by pre-stimulation power in the frequency band of the endogenous oscillation. Mean
252 gamma power was calculated in the center frequency of oscillation (5 Hz window). To quantify
253 the slope of post-stimulation, a line was fitted within a 300 ms window immediately after
254 stimulation turned off using the “polyfit” function in MATLAB 2016b (MathWorks Inc, Natick, MA,
255 USA). All the results are reported as mean \pm SEM; n= number of slices. For statistical analysis
256 paired t-test was used to compare post and pre stimulation in each electric field intensity and

257 significance level (p) was corrected using Bonferroni for multiple (e.g. for four comparisons
258 made in each experiment $p < 0.0125$ was considered significant). All the analysis was performed
259 in R (RStudio, Inc., Boston, MA).

260

261 **Results**

262 *Effect of kHz stimulation on hippocampal field potentials in CA1*

263

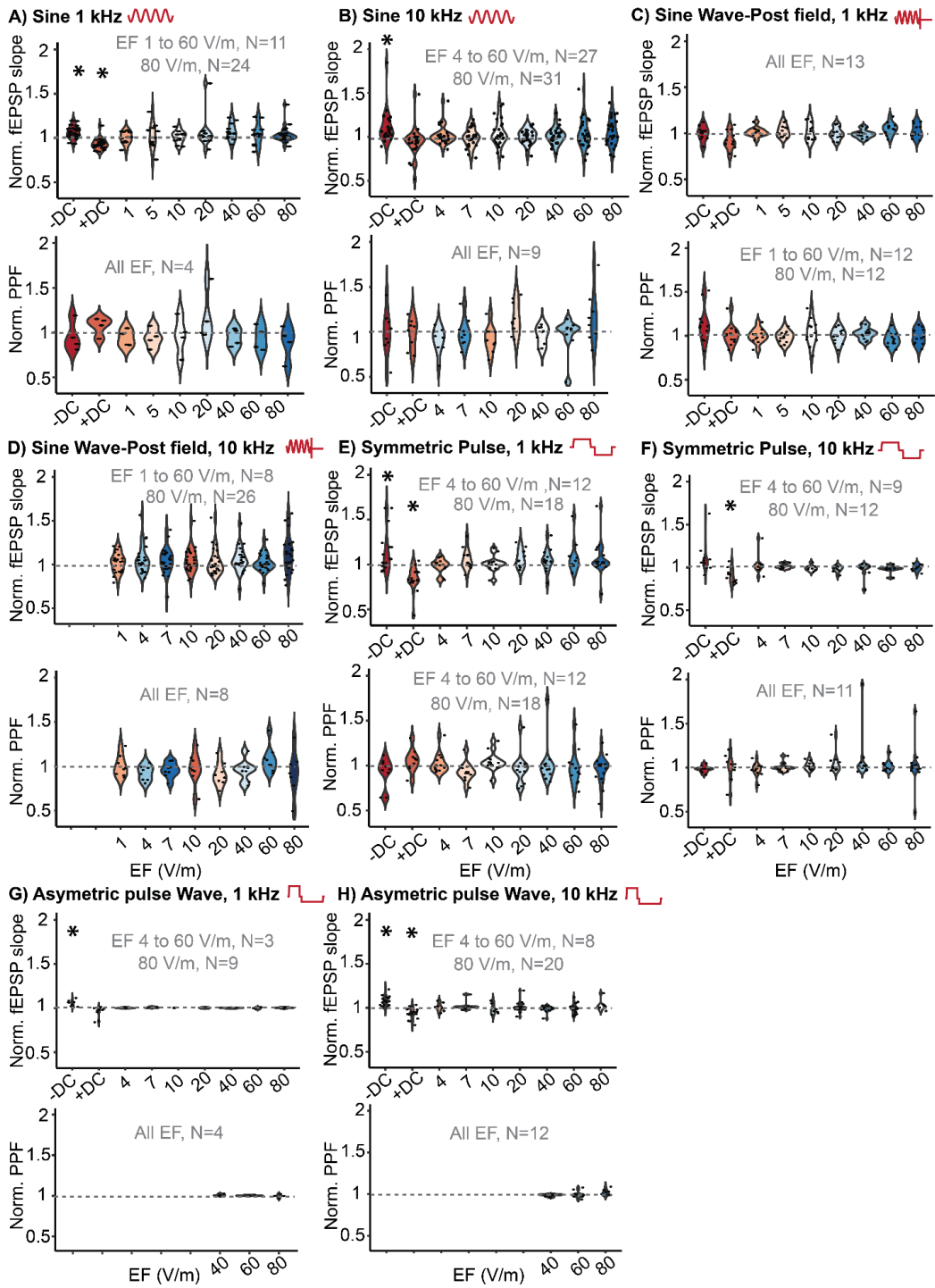
264 Field excitatory post-synaptic potentials (fEPSP) measured at dendrites reflect the
265 aggregate post-synaptic current entering to a population of neurons, which is a measure of
266 synaptic input. Field EPSPs are sensitive to low-frequency electric fields (Bikson et al., 2004;
267 Lafon et al., 2017). Using rat hippocampal slice preparation, we tested the acute and long-term
268 effects of uniform unmodulated kHz electric fields on synaptic efficacy with electric field direction
269 in parallel or perpendicular to primary somato-dendritic axis (Bikson et al., 2004). The effects of
270 DC electric field were also assessed as within-slice positive controls. Field EPSPs were evoked
271 in CA1 region of rat hippocampus by activating the Schaffer collateral pathway. Unless
272 otherwise stated, changes in fEPSP slope from electric field application were calculated as a
273 ratio of slope during electric field application versus control (i.e. no stimulation). Paired pulse
274 facilitation (PPF) which is a measure of short-term synaptic plasticity was used in our recording
275 and was calculated as the ratio of the second fEPSP slope to the first (50 ms inter-pulse
276 interval) in each condition. Unless otherwise stated, results are reported as mean \pm SEM and
277 stimulation were applied for 1 s in all acute experiments and 30 min in long-term experiments.

278 When electric fields were applied in the radial direction (electric field parallel to the
279 somato-dendritic axis of CA1 pyramidal neurons), sinusoidal stimulation with 1 kHz did not
280 produce significant effects ($F(6, 75) = 0.5835$, ns) in any of intensities tested (1, 5, 10, 20, 40, 60,
281 80 V/m). However, DC stimulation significantly modulated fEPSP slope (-DC (1.06 ± 0.014 ,

282 N=24, $p < 0.01$) +DC (0.932 ± 0.0127 , N=24, $p < 0.01$). Neither DC nor 1 kHz sinusoidal
283 stimulation affected PPF. Increasing stimulation frequency from 1 kHz to 10 kHz (fEPSP, 10
284 kHz: (F(6,160)=0.86, ns, PPF, 10 kHz : (F(6,55)=2.8, ns)), or changing recording time from during
285 stimulation to immediately after the field was turned off (fEPSP, 1 kHz F(6,66)=1.21, ns; PPF
286 F(6,66)=0.88, ns; fEPSP, 10 kHz F(7,175)= 2.2, ns, PPF F(7,47)=1.316 , ns) did not modulate
287 fEPSP over the range of electric field intensities tested (Figure 2.B, C).

288 Symmetric and asymmetric charge-balanced waveforms are ubiquitous in implanted
289 stimulators including DBS and SCS. Stimulation with radially-directed symmetric pulse
290 waveforms at 1 kHz and 10 kHz electric fields did not modulate fEPSP (1kHz, F(6,73)=0.788,ns;
291 10kHz, F(6,50)=1.03, ns) or PPF (1kHz, F(6,72)=1.30, ns; 10kHz, F(6,61)=0.68, ns) (Figure 2.E,
292 F). Radially directed electric fields with asymmetric pulse waveform also did not modulate
293 fEPSP or PPF regardless of frequency (Figure 2. G, H) (fEPSP: 1kHz, F(6,15)=0.63, ns; 10kHz,
294 F(6,84)=1.022, ns; PPF: 1kHz, F(2,9)=0.72, ns; 10kHz, F(2,32)=0.86,ns).

295

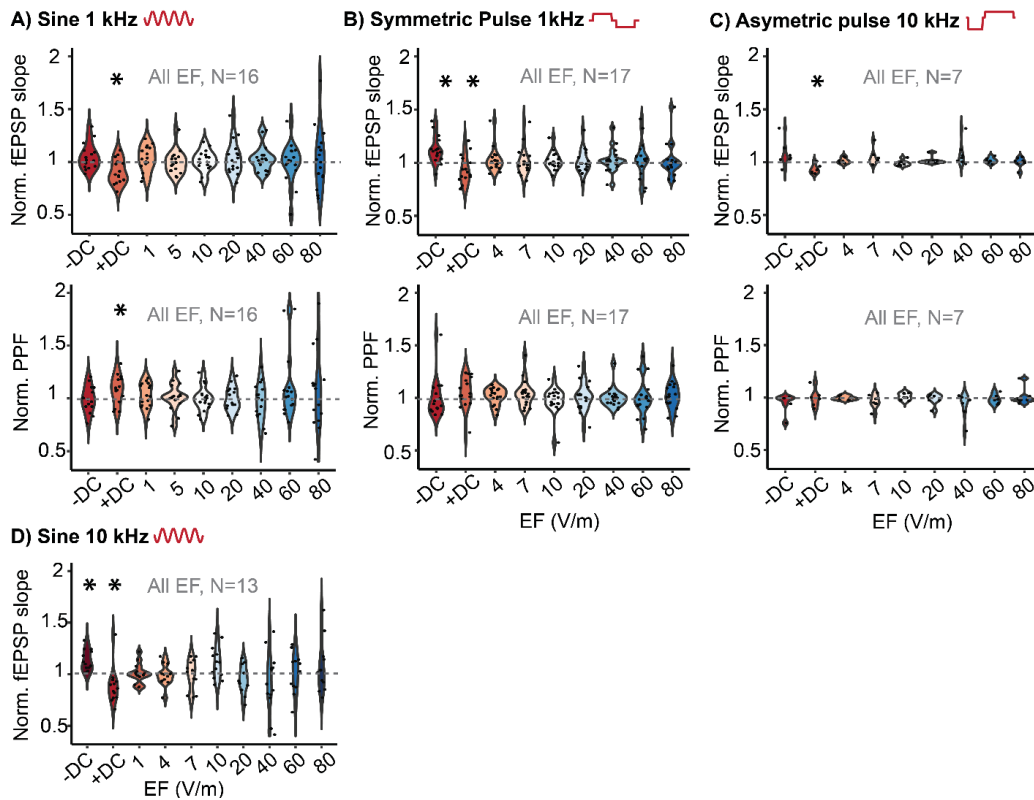


297 **Figure 2:** Acute effect of direct current and high frequency electrical stimulation in radial electric field. **(A)** Normalized
298 slope of fEPSP and paired-pulse facilitation (PPF) during positive and negative 40 V/m DC and 1 kHz sinusoidal
299 stimulation. **(B)** Normalized slope of fEPSP and paired-pulse facilitation (PPF) during positive and negative 40 V/m
300 DC and 10 kHz sinusoidal stimulation. **(C)** Normalized slope of fEPSP and paired-pulse facilitation (PPF) immediately
301 after 1 kHz sinusoidal stimulation (post-field). **(D)** Normalized slope of fEPSP and paired-pulse facilitation (PPF)
302 immediately after positive and negative 40 V/m DC and 10 kHz sinusoidal stimulation (post-field). **(E)** Normalized
303 slope of fEPSP and paired-pulse facilitation (PPF) during positive and negative 40 V/m DC and 1 kHz symmetric
304 pulse waveform stimulation. **(F)** Normalized slope of fEPSP and paired-pulse facilitation (PPF) during positive and
305 negative 40 V/m DC and 10 kHz symmetric pulse waveform stimulation. **(G)** Normalized slope of fEPSP and paired-
306 pulse facilitation (PPF) during positive and negative 40 V/m DC and 1 kHz Asymmetric pulse waveform stimulation.
307 **(H)** Normalized slope of fEPSP and paired-pulse facilitation (PPF) during positive and negative 40 V/m DC and 10
308 kHz Asymmetric pulse waveform stimulation. Black circles indicate each data point. Recording frame was 30 s long in
309 all the acute experiments. Stimulation was applied for 1 s in the middle of the recording frame (14.5 -15.5 s). Each
310 data point represents average of 3-15 repetition. N, the number of hippocampal slices in each intensity. EF: Electric
311 Field. * $p < 0.05$.

312

313 When electric field was applied in tangential direction (i.e. perpendicular to somato-
314 dendritic axis of CA1 pyramidal neurons), sinusoidal waveform (1kHz: fEPSP,
315 $F(6,105)=0.231, ns$, PPF, $F(5,90)=0.58, ns$; 10 kHz: fEPSP $F(7,83)=1.52, ns$) (Figure 3.A, D),
316 symmetric (1 kHz: fEPSP, $F(6,96)=0.08, ns$, PPF, $F(6,96)=0.52, ns$) and asymmetric waveforms
317 (10 kHz: fEPSP, $F(6,36)=1.71, ns$, PPF, $F(6,41)=1.30, ns$), at 1 kHz or 10 kHz, did not modulate
318 fEPSPs.

319



320

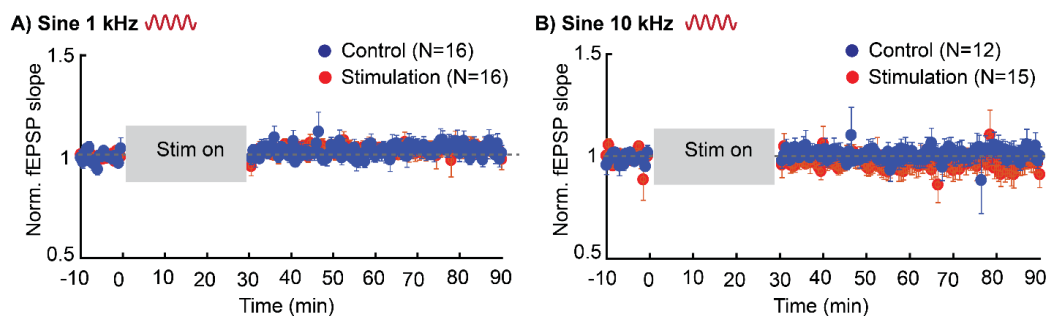
321 **Figure 3:** Acute effect of direct current and high frequency stimulation in tangential direction. **(A)** Normalized slope of
 322 fEPSP and paired-pulse facilitation (PPF) during positive and negative 40 V/m DC and 1 kHz sinusoidal stimulation.
 323 **(B)** Normalized slope of fEPSP and paired-pulse facilitation (PPF) during positive and negative 40 V/m DC and 1 kHz
 324 symmetric pulse waveform. **(C)** Normalized slope of fEPSP and paired-pulse facilitation (PPF) during positive and
 325 negative 40 V/m DC and 10 kHz asymmetric pulse waveform. **(D)** Normalized slope of fEPSP during positive and
 326 negative 40 V/m DC and 10 kHz asymmetric sine waveform. Colored circles indicate different data point. Black line:
 327 mean, light grey box: standard deviation and dark grey boxes demonstrate SEM for each experiment. N, the number
 328 of hippocampal slices. *EF: Electric Field* * $p < 0.05$.

329

330 Whereas all the prior results used brief application of electric fields, we further tested if
 331 stimulation for a longer period (i.e. 30 min) can induce lasting effects on fEPSP under the
 332 hypothesis that small effects could be amplified with longer stimulation duration. Stable baseline

333 fEPSP was recorded every 30 s for over 20 min before stimulation and 60 min after stimulation.
 334 Electrical stimulation was done using sinusoidal 1 and 10 kHz stimulation with 80 V/m electric
 335 field intensity (Figure 4) and effect on fEPSP was analyzed for condition (i.e. sham, stimulation)
 336 and time (i.e. immediately, 30 and 60 minutes after termination of stimulation). A repeated
 337 measure ANOVA revealed no significant effects for stimulation condition (1 kHz : $F(1,27)=0.113$,
 338 $p=0.739$; 10 kHz: $F(1,23)=0.09$, $p=0.767$), time (1 kHz: $F(2,54)=0.024$, $p=0.97$; 10 kHz:
 339 $F(2,46)=1.01$, $p=0.375$) and no interactions (1 kHz: $F(2,54)=1.01$, $p=0.37$; 10 kHz: $F(2,46)=1.92$
 340 , $p=0.158$).

341



342

343 **Figure 4:** Long-term effect of kHz stimulation on synaptic efficacy. **(A)** Normalized field EPSP slope in response to 30
 344 minutes stimulation (between 0 to 30) 1 kHz sine waveform, 80 V/m in radial direction after at least 20 minutes stable
 345 baseline. Follow up recording continued for 60 minutes after stimulation. **(B)** Normalized field EPSP slope in
 346 response to 30 minutes 10 kHz sine waveform, 80 V/m in radial direction. Error bars indicates standard error of
 347 mean. N, number of slices. Blue (control), red (stimulation).

348

349 Bayesian analysis for supporting null hypothesis:

350 Since these negative results may support either evidence of absence (provide support
 351 for null hypothesis) or absence of evidence due to lack of statistical power, we performed Bayes
 352 factor hypothesis testing for fEPSP evoked during 80 V/m stimulation applied in radial direction

353 (parallel to somato-dendritic axis of pyramidal neurons) for 1 and 10 kHz sinusoidal, symmetric
354 and asymmetric waveforms. Moderate evidence was found for the absence of effect using 80
355 V/m, 10 kHz sinusoidal waveform, meaning that the observed data was ~ 3x more likely to be
356 under the null hypothesis than the alternative ($BF_{+0}=0.34$ with median posterior $\delta =0.187$, 95%
357 $CI=[-0.177,0.560]$), and anecdotal evidence for absence of effect in 1 kHz sinusoidal stimulation,
358 meaning that the observed data was 1.67x more likely to be under the null hypothesis than the
359 alternative ($BF_{+0}=0.63$ with median posterior $\delta = -0.334$, 95% $CL=[-0.924,0.210]$).

360 Using Bayes factor in symmetric pulse waveforms showed that data observed in 10 kHz
361 is ~ 3x more likely to be under the null hypothesis; providing moderate evidence for null
362 ($BF_{+0}=0.33$ with median posterior $\delta =-0.122$, 95% $CL=[-0.665,0.402]$) whereas observed data in
363 1 kHz the data provided anecdotal evidence for null hypothesis: data was 1.33x more likely to
364 be under the null hypothesis ($BF_{+0}=0.75$ with median posterior $\delta =0.369$, 95% $CI=[-$
365 $0.162,0.943]$). The data observed in during asymmetric pulse stimulation provided anecdotal
366 evidence for both 1 and 10 kHz stimulation, meaning the observed data was 2.13x and 1.23x
367 more likely to be under the null hypothesis, respectively (1 kHz: $BF_{+0}=0.47$ with median
368 posterior $\delta =-0.081$, 95% $CL=[-1.004,0.789]$, 10 kHz: $BF_{+0}=0.81$ with median posterior $\delta =-0.42$,
369 95% $CL=[-0.216,1.143]$).

370 Bayesian repeated measure ANOVA revealed strong evidence (1kHz: $BF=0.1$; 10 kHz:
371 $BF=0.3$) in support of the null hypothesis regarding effect of time (effect on EPSP immediate, 30
372 min or 60 min after stimulation) and moderate evidence (1 kHz: $BF=0.4$, 10 kHz: $BF=0.3$) in
373 support of the null hypothesis regarding effect of stimulation condition (i.e. sham vs stimulation
374 on). Regarding interactions, Bayesian analysis revealed moderate and anecdotal evidence in
375 support of the null hypothesis for 1 kHz and 10 kHz, respectively (1 kHz: $BF=0.35$, 10 kHz:
376 $BF=0.8$).

377

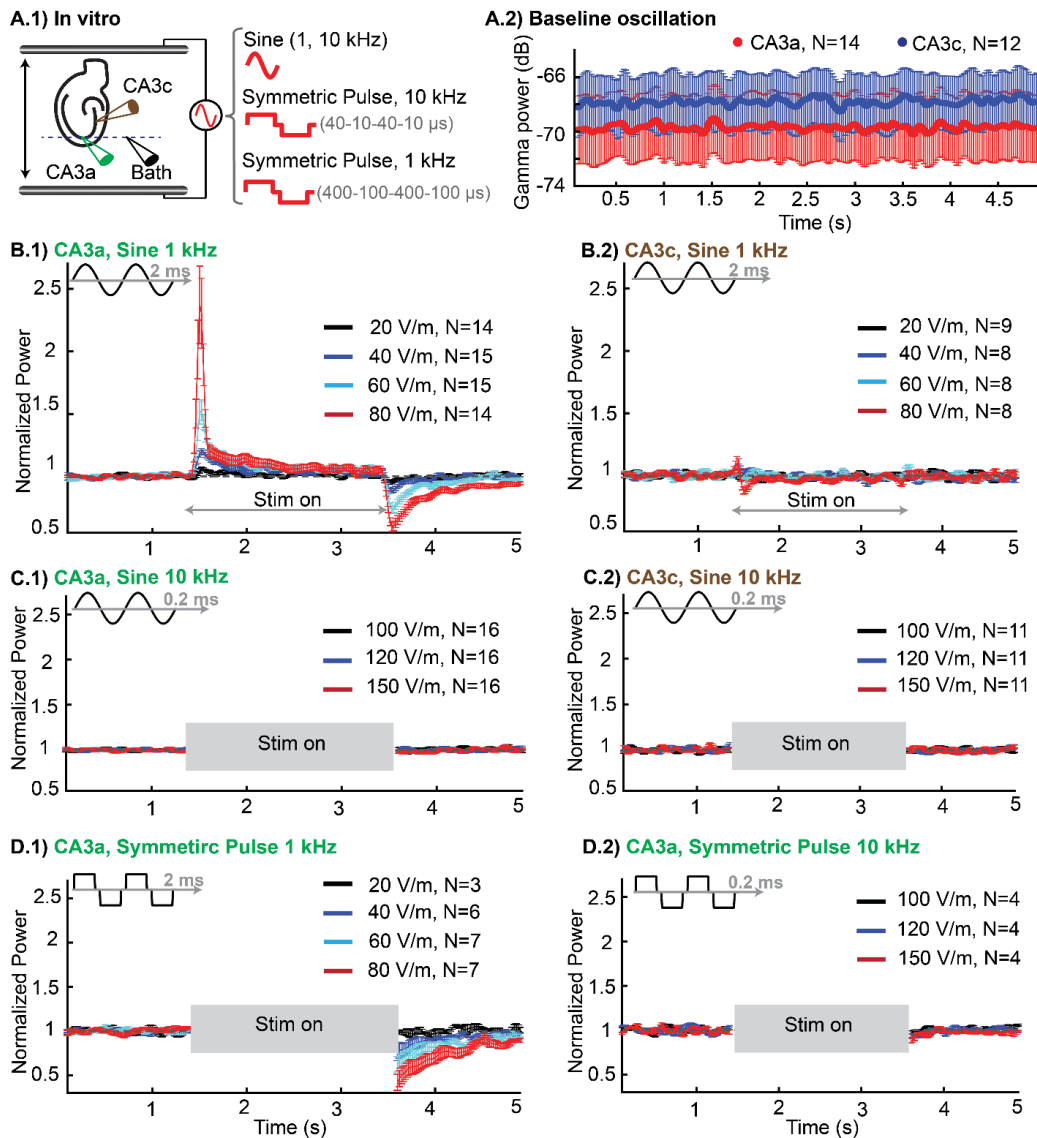
378

379 *Effect of kHz stimulation on hippocampal gamma oscillations*

380 Uniform unmodulated 1 and 10 kHz electric fields were applied across hippocampal
381 slices exhibiting gamma oscillations under carbachol perfusion (Figure 5.A.1). Oscillations were
382 typically stable over ~3 hours and experiments started after verifying stabilization of gamma
383 oscillation power. We evaluated the sensitivity of gamma network activity to stimulation with kHz
384 electric fields. Each stimulation was 2 s long and signals were recorded in frames of 5 s (acute
385 effect, 5 s frame length (1.5 s pre, 2 s stim, 1.5 post), 80-100 frames per slice). Gamma
386 oscillation was recorded from both CA3a and CA3c region of hippocampus. There was no
387 significant difference in baseline gamma power between the two recording locations (CA3a,
388 N=14; CA3c, N=12, ns) (Figure 5.A.2).

389 Consistent with previous reports (Esmailpour et al., 2020; Reato et al., 2010), low kHz
390 stimulation generated transient effect at the onset of stimulation as well as a sustained effect in
391 CA3a region (Figure 5.B.1). This muted sustained effect is presumably reflecting homeostatic
392 network regulation to bring the network back toward equilibrium (e.g. baseline oscillatory level).
393 Moreover, stimulation produced a post-stimulation suppression of oscillation (see below) which
394 is a marker of network rebound from homeostatic adaptation (Reato et al., 2010). Gamma
395 oscillation recorded from CA3c region was not modulated during stimulation (Figure 5.B.2),
396 highlighting the importance of electric field direction relative to somato-dendritic axis of
397 pyramidal neurons for somatic polarization (Radman et al., 2009).

398



399
 400 **Figure 5:** Sensitivity of hippocampal gamma oscillations during application of 1 and 10 kHz sinusoidal and square
 401 waveform stimulation. **(A)** Rat in vitro model of gamma oscillation. A.1, Experimental setup: spatially uniform electric
 402 field was applied across hippocampal slices in an interface chamber. Recording of gamma oscillation from CA3a and
 403 CA3c relative to bath electrode to minimize stimulation noise. A.2, Mean (\pm SEM) of baseline gamma power (in dB) for
 404 CA3a and CA3c across slices. **(B)** Mean (\pm SEM) of normalized gamma power across slices for 2 seconds of
 405 stimulation (between 1.5 and 3.5 s) using 1 kHz sinusoidal waveform with different field intensities recorded from
 406 CA3a (B.1) and CA3c (B.2). **(C)** Mean (\pm SEM) of normalized gamma power across slices for 2 seconds of stimulation

407 (between 1.5 and 3.5 s) using 10 kHz sinusoidal waveform with different field intensities recorded from CA3a (C.1)
408 and CA3c (C.2). (D) Mean (\pm SEM) of normalized gamma power across slices for 2 seconds of stimulation (between
409 1.5 and 3.5 s) using 1 kHz symmetric pulse waveform with different field intensities (D.1) and 10 kHz symmetric pulse
410 waveform with different field intensities (D.2) recorded from CA3a region of rat hippocampus. N, number of slices.

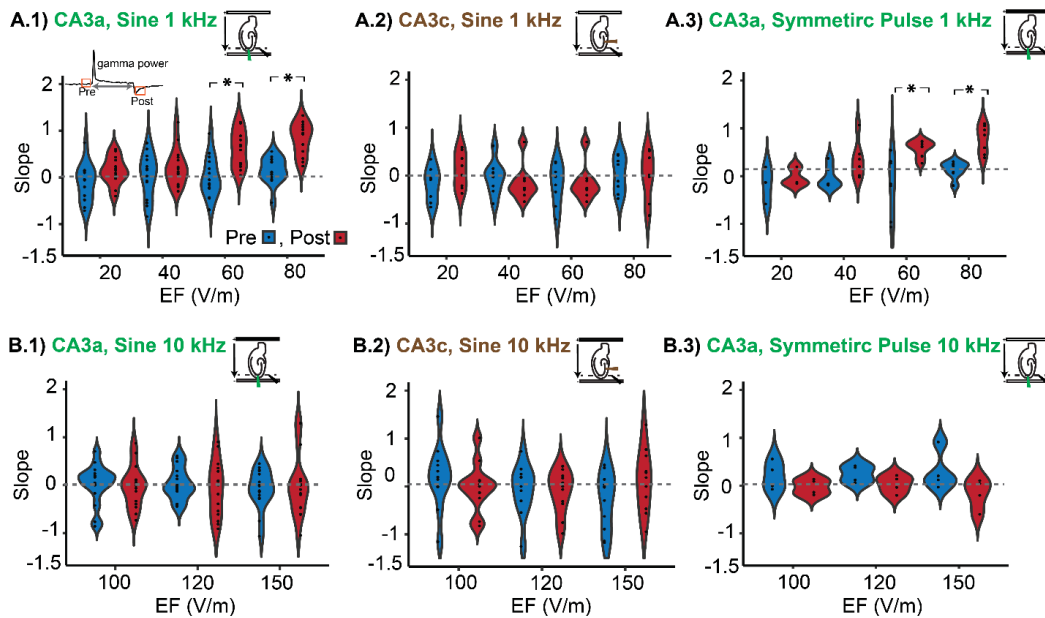
411

412 Due to technical concerns of reliably removing stimulation artifact during 10 kHz
413 sinusoidal stimulation and symmetric pulse waveforms, oscillation data was analyzed comparing
414 only the pre and post stimulation time windows (Figure 5 .C, D). We defined slope of average
415 gamma power (see methods) measured in 300 ms window immediately after termination of
416 stimulation as a metric to quantify post-stimulation suppression (Figure. 6).

417 Significant post-stimulation suppression was detected using 1 kHz sinusoidal waveform
418 with field intensities ≥ 60 V/m in CA3a region (gamma power slope: 60 V/m, Post: 0.62 ± 0.010 ,
419 Pre: $8.5 \cdot 10^{-4} \pm 0.11$, N=15, $p < 0.001$; 80 V/m Post: 0.83 ± 0.09 , Pre: 0.15 ± 0.074 , N=14,
420 $p < 0.001$) (Figure 6.A.1), however in CA3c region, no change was detected in slope of gamma
421 power immediately after stimulation (Figure 6.A.2). Similarly, symmetric pulse 1 kHz stimulation
422 using intensities ≥ 60 V/m induced significant rebound after stimulation (gamma power slope: 60
423 V/m, Post: 0.58 ± 0.06 , Pre: -0.15 ± 0.23 , N=7, $p < 0.01$; 80 V/m, Post: 0.77 ± 0.11 , Pre: $0.13 \pm$
424 0.64 , N=7, $p < 0.01$) (Figure 6.A.3). Increasing stimulation frequency from 1 to 10 kHz abolished
425 the effect. No effect was observed in 10 kHz symmetric pulse and sinusoidal stimulation using
426 post-stimulation suppressions as an index even when testing still higher electric field strength
427 (i.e. 100, 120 and 150 V/m) (Figure 6.B).

428

429



430

431 **Figure 6:** Post-stimulation suppression of average gamma oscillation power. **(A)** Slope of mean gamma oscillation
 432 power (illustrated in figure 5) measured from 300 ms window immediately before and after 2 s of stimulation using 1
 433 kHz sine waveform recorded from CA3a (A.1) and CA3c (A.2) and symmetric pulse waveform electrical stimulation
 434 recorded from CA3a region (A.3). **(B)** Slope of gamma oscillation immediately before and after 10 kHz stimulation
 435 recorded from CA3a (B.1) and CA3c (B.2) using sinusoidal and symmetric pulse waveform recorded from CA3c
 436 region (B.3). Red, post stimulation gamma slope. Blue, pre stimulation gamma slope. Black line: mean, light grey box:
 437 standard deviation and dark grey boxes demonstrate standard error of mean for each experiment.

438

439

440

441

442

443

444

445

446 **Discussion**

447

448 There is a long-standing interest in explaining neuronal responses to kHz range
449 electrical stimulation (Katz, 1939; Ward, 2009) with many results still inconclusive or without
450 satisfactory theoretical treatment. Various forms of kHz neuromodulation techniques have
451 shown promise in managing chronic pain (Al-Kaisy et al., 2015; Thomson et al., 2018) improving
452 motor function in Parkinson's disease (Harmsen et al., 2019) and modulating excitability of
453 human motor cortex (Antal and Paulus, 2013; Chaieb et al., 2011; Terney et al., 2008).
454 Variations of kHz stimulation (electrode position, pulsed/sinusoidal waveforms) has been
455 characterized in a broad range of applications including physiotherapy (Medeiros et al., 2017;
456 Ward, 2009), ceasing abnormal neuronal activity (Kilgore and Bhadra, 2014; Lempka et al.,
457 2015; Pelot and Grill, 2020) or generating spontaneous or asynchronous firing (Crosby et al.,
458 2017; Litvak et al., 2003; Rubinstein et al., 1999). In contrast, it is a fundamental property of
459 cells that the parallel leak conductance and capacitance of outer membrane forms an equivalent
460 of a filter that attenuates neuronal responses to inputs with high frequency components. This
461 intrinsic low pass filtering property of neuronal membrane explains various electrophysiological
462 finding at the cellular and neuronal network level on limited sensitivity to kHz electric fields
463 (Deans et al., 2007; Reato et al., 2010) - though once polarized, ions channel have some
464 kinetics with sub-ms time constants (Zhang et al., 2006; Zhao et al., 2014). At the same time,
465 some application using Amplitude-Modulated (AM) kHz stimulations are based on the
466 assumption neurons are insensitive to the unmodulated kilohertz component (Goats, 1990;
467 Grossman et al., 2017; Ward, 2009). We therefore set out to clarify the sensitivity of the brain to
468 unmodulated, uniform, 1 or 10 kHz sinusoidal (e.g. single frequency band) fields between 1 and
469 150 V/m.

470 The acute brain slice model has been extensively used as a model system to screen for
471 effects of a broad range of stimulation waveform and intensities, including sub-threshold fields
472 (Bikson et al., 2004; Jackson et al., 2016; Rahman et al., 2017; Rahman et al., 2013) and is
473 generally among the most characterized experimental system in neuroscience (Ranieri et al.,
474 2012). Consistent with screening for a broad range of possible effects, single and paired
475 fEPSPs are sensitive to changes either in pre- or post-synaptic excitability. Oscillations are
476 similarly highly sensitive to changes in excitatory and inhibitory cellular function through
477 mechanism of amplification specific to network's architecture and level of activity (Jackson et al.,
478 2016; Reato et al., 2010, 2013). Furthermore, field measures are insensitive to intracellular
479 artifacts specific to kHz fields (FallahRad et al., 2019; Lesperance et al., 2018). A change in
480 fEPSP or oscillations in response to kHz electric fields are thus robust and broad indicators of
481 changes in brain function – which, if positive, can then be followed by more specific testing to
482 identify cellular targets.

483 We systematically evaluated responses to a range of waveforms (sinusoidal, symmetric,
484 asymmetric pulses), intensities, 1 kHz and 10 kHz frequencies, electric field direction (radial,
485 tangential), stimulation duration (30 s typical, 30 min), and during and post-field effects. While
486 impractical to test all combinations, our overall experimental strategy was intended to identify
487 responses. We focused (number of slices) on 80 V/m but tested a range of intensities in case
488 responses are not monotonic. Given established sensitivity to DC fields of slice prep neurons
489 (Bikson et al., 2004; Jackson et al., 2016), we conducted within-slice positive controls for
490 general sensitivity to electric fields. By any measure, field EPSPs were not modulated by kHz
491 waveform tested, regardless of intensity (up to 80 V/m), waveform, direction, or timing. 1 kHz
492 but not 10 kHz electric field modulated ongoing network oscillations. The intensity required for 1
493 kHz electric fields to modulate gamma oscillation was substantially higher than for low-
494 frequency (e.g. ~100 Hz) fields (Esmaeilpour et al., 2020). This overall lack of sensitivity is

495 consistent with prior kHz-stimulation mechanistic studies (Couto and Grill, 2016; Esmailpour et
496 al., 2020; Lempka et al., 2015; Negahbani et al., 2018) and the established low-pass filtering
497 characteristics of neuronal membranes to electrical stimulation (Deans et al., 2007; Reato et al.,
498 2013).

499 Our results are limited by several factors. It is never possible to exclude beta errors,
500 though our use of a high SNR experimental system, with multiple slices and numerous
501 repetitions per condition per slice, as well as within slice positive DC controls, together suggest
502 such undetected effects would be variable or small in any case. Alternative mechanisms of
503 electric fields such as ion concentration changes (Bikson et al., 2001; Shapiro et al., 2020;
504 Wang et al., 2020), fiber block (Patel and Butera, 2015; Shapiro et al., 2020; Zhang et al., 2006;
505 Zhao et al., 2014) and transverse axonal polarization (Wang et al., 2018) are suggested for
506 kilohertz stimulation at very high intensities. However these very high intensities are not
507 expected in existing clinical applications, such as SCS, with targeted tissue some mm away
508 from the electrode (Idlett et al., 2019; Lempka et al., 2015). As emphasized throughout this
509 paper, these results are limited by any biophysical features absent from our experimental model
510 system. Effective kHz stimulation with intensities comparable to these clinical applications would
511 require a transduction mechanism with an especially fast time constant that is absent in acute
512 rodent brain slice.

513 Following the quasi-uniform assumption (Bikson et al., 2013; Bikson et al., 2015; Khadka
514 et al., 2019), we applied uniform fields, leaving open the possibility that geometry-sensitive
515 effects were missed (Idlett et al., 2019). Our results are limited to the intensities and specific
516 waveforms tested, though a range of pulse-shapes were considered. We cannot consider
517 possible mechanisms not captured by the hippocampal brain slice, such as a highly sensitive
518 subtype of neurons (Lee et al., 2020; Litvak et al., 2003; Rubinstein et al., 1999), vascular

519 responses (Cancel et al., 2018) or temperature (Zannou et al., 2019a; Zannou et al., 2019b); the
520 latter in fact increases with kHz frequency.

521

522 **Disclosures**

523 The City University of New York holds patents on brain stimulation with MB as inventor. MB has
524 equity in Soterix Medical Inc. MB consults, received grants, assigned inventions, and/or serves
525 on the SAB of Boston Scientific, GlaxoSmithKline, Mecta, Halo Neuroscience, X.

526 Other authors reported no conflict of interest.

527

528 **Acknowledgement**

529 MB is supported by grants from the National Institutes of Health: R01NS101362 (MB),
530 R01NS095123 (MB), R01NS112996 (MB), R01MH111896 (MB), R01MH109289 (MB).

531

532 **Reference**

533 Al-Kaisy, A., Palmisani, S., Smith, T., Harris, S., Pang, D., 2015. The use of 10-kilohertz spinal cord
534 stimulation in a cohort of patients with chronic neuropathic limb pain refractory to medical
535 management. *Neuromodulation: Technology at the Neural Interface* 18, 18-23.
536 Antal, A., Paulus, W., 2013. Transcranial alternating current stimulation (tACS). *Frontiers in human*
537 *neuroscience* 7, 317.
538 Bikson, M., Dmochowski, J., Rahman, A., 2013. The “quasi-uniform” assumption in animal and
539 computational models of non-invasive electrical stimulation. *Brain stimulation* 6, 704.
540 Bikson, M., Inoue, M., Akiyama, H., Deans, J.K., Fox, J.E., Miyakawa, H., Jefferys, J.G., 2004. Effects of
541 uniform extracellular DC electric fields on excitability in rat hippocampal slices in vitro. *The Journal of*
542 *physiology* 557, 175-190.
543 Bikson, M., Lian, J., Hahn, P.J., Stacey, W.C., Sciortino, C., Durand, D.M., 2001. Suppression of
544 epileptiform activity by high frequency sinusoidal fields in rat hippocampal slices. *The Journal of*
545 *physiology* 531, 181.
546 Bikson, M., Rahman, A., 2013. Origins of specificity during tDCS: anatomical, activity-selective, and input-
547 bias mechanisms. *Frontiers in human neuroscience* 7, 688.

- 548 Bikson, M., Truong, D.Q., Mourdoukoutas, A.P., Abozeria, M., Khadka, N., Adair, D., Rahman, A., 2015.
549 Modeling sequence and quasi-uniform assumption in computational neurostimulation. *Progress in brain*
550 *research*. Elsevier, pp. 1-23.
- 551 Bradley, K., Redwood City, C., 2017. Paresthesia-Independence: An Assessment of Technical Factors
552 Related to 10 kHz Paresthesia-Free Spinal Cord Stimulation. *Pain Physician* 20, 331-341.
- 553 Cancel, L.M., Arias, K., Bikson, M., Tarbell, J.M., 2018. Direct current stimulation of endothelial
554 monolayers induces a transient and reversible increase in transport due to the electroosmotic effect.
555 *Scientific Reports* 8, 1-13.
- 556 Chaieb, L., Antal, A., Paulus, W., 2011. Transcranial alternating current stimulation in the low kHz range
557 increases motor cortex excitability. *Restor Neurol Neurosci* 29, 167-175.
- 558 Couto, J., Grill, W.M., 2016. Kilohertz frequency deep brain stimulation is ineffective at regularizing the
559 firing of model thalamic neurons. *Frontiers in computational neuroscience* 10, 22.
- 560 Crosby, N.D., Janik, J.J., Grill, W.M., 2017. Modulation of activity and conduction in single dorsal column
561 axons by kilohertz-frequency spinal cord stimulation. *Journal of neurophysiology* 117, 136-147.
- 562 Deans, J.K., Powell, A.D., Jefferys, J.G., 2007. Sensitivity of coherent oscillations in rat hippocampus to AC
563 electric fields. *The Journal of physiology* 583, 555-565.
- 564 Dmochowski, J., Bikson, M., 2017. Noninvasive Neuromodulation Goes Deep. *Cell* 169, 977-978.
- 565 Dowden, B.R., Wark, H.A., Normann, R.A., 2010. Muscle-selective block using intrafascicular high-
566 frequency alternating current. *Muscle Nerve* 42, 339-347.
- 567 Esmaeilpour, Z., Kronberg, G., Reato, D., Parra, L.C., Bikson, M., 2020. Temporal interference stimulation
568 targets deep brain regions by modulating neural oscillations. *bioRxiv*, 2019.2012.2025.888412.
- 569 FallahRad, M., Zannou, A.L., Khadka, N., Prescott, S.A., Ratte, S., Zhang, T., Esteller, R., Hershey, B.,
570 Bikson, M., 2019. Electrophysiology equipment for reliable study of kHz electrical stimulation. *The*
571 *Journal of physiology* 597, 2131-2137.
- 572 Fritsch, B., Reis, J., Martinowich, K., Schambra, H.M., Ji, Y., Cohen, L.G., Lu, B., 2010. Direct current
573 stimulation promotes BDNF-dependent synaptic plasticity: potential implications for motor learning.
574 *Neuron* 66, 198-204.
- 575 Fröhlich, F., McCormick, D.A., 2010. Endogenous electric fields may guide neocortical network activity.
576 *Neuron* 67, 129-143.
- 577 Gluckman, B.J., Netoff, T.I., Neel, E.J., Ditto, W.L., Spano, M.L., Schiff, S.J., 1996. Stochastic resonance in
578 a neuronal network from mammalian brain. *Physical Review Letters* 77, 4098.
- 579 Goats, G., 1990. Interferential current therapy. *British journal of sports medicine* 24, 87.
- 580 Grossman, N., Bono, D., Dedic, N., Kodandaramaiah, S.B., Rudenko, A., Suk, H.J., Cassara, A.M., Neufeld,
581 E., Kuster, N., Tsai, L.H., Pascual-Leone, A., Boyden, E.S., 2017. Noninvasive Deep Brain Stimulation via
582 Temporally Interfering Electric Fields. *Cell* 169, 1029-1041.e1016.
- 583 Harmsen, I.E., Lee, D.J., Dallapiazza, R.F., De Vloo, P., Chen, R., Fasano, A., Kalia, S.K., Hodaie, M., Lozano,
584 A.M., 2019. Ultra-high-frequency deep brain stimulation at 10,000 Hz improves motor function. *Mov*
585 *Disord* 34, 146-148.
- 586 Idlett, S., Halder, M., Zhang, T., Quevedo, J., Brill, N., Gu, W., Moffitt, M., Hochman, S., 2019. Assessment
587 of axonal recruitment using model-guided preclinical spinal cord stimulation in the ex vivo adult mouse
588 spinal cord. *Journal of neurophysiology* 122, 1406-1420.
- 589 Jackson, M.P., Rahman, A., Lafon, B., Kronberg, G., Ling, D., Parra, L.C., Bikson, M., 2016. Animal models
590 of transcranial direct current stimulation: Methods and mechanisms. *Clinical Neurophysiology* 127,
591 3425-3454.
- 592 Jefferys, J., 1981. Influence of electric fields on the excitability of granule cells in guinea-pig hippocampal
593 slices. *The Journal of physiology* 319, 143.

- 594 Kabakov, A.Y., Muller, P.A., Pascual-Leone, A., Jensen, F.E., Rotenberg, A., 2012. Contribution of axonal
595 orientation to pathway-dependent modulation of excitatory transmission by direct current stimulation
596 in isolated rat hippocampus. *Journal of neurophysiology* 107, 1881-1889.
- 597 Kapural, L., Yu, C., Doust, M.W., Gliner, B.E., Vallejo, R., Sitzman, B.T., Amirdelfan, K., Morgan, D.M.,
598 Brown, L.L., Yearwood, T.L., 2015. Novel 10-kHz High-frequency Therapy (HF10 Therapy) Is Superior to
599 Traditional Low-frequency Spinal Cord Stimulation for the Treatment of Chronic Back and Leg PainThe
600 SENZA-RCT Randomized Controlled Trial. *The Journal of the American Society of Anesthesiologists* 123,
601 851-860.
- 602 Katz, B., 1939. Nerve excitation by high-frequency alternating current. *The Journal of physiology* 96, 202.
- 603 Keysers, C., Gazzola, V., Wagenmakers, E.-J., 2020. Using Bayes factor hypothesis testing in neuroscience
604 to establish evidence of absence. *Nature Neuroscience* 23, 788-799.
- 605 Khadka, N., Harmsen, I.E., Lozano, A.M., Bikson, M., 2020. Bio-Heat Model of Kilohertz-Frequency Deep
606 Brain Stimulation Increases Brain Tissue Temperature. *Neuromodulation*.
- 607 Khadka, N., Truong, D.Q., Williams, P., Martin, J.H., Bikson, M., 2019. The Quasi-uniform assumption for
608 Spinal Cord Stimulation translational research. *Journal of neuroscience methods* 328, 108446.
- 609 Kilgore, K.L., Bhadra, N., 2014. Reversible nerve conduction block using kilohertz frequency alternating
610 current. *Neuromodulation: Technology at the Neural Interface* 17, 242-255.
- 611 Korte, M., Carroll, P., Wolf, E., Brem, G., Thoenen, H., Bonhoeffer, T., 1995. Hippocampal long-term
612 potentiation is impaired in mice lacking brain-derived neurotrophic factor. *Proceedings of the National*
613 *Academy of Sciences* 92, 8856-8860.
- 614 Kronberg, G., Bridi, M., Abel, T., Bikson, M., Parra, L.C., 2017. Direct current stimulation modulates LTP
615 and LTD: activity dependence and dendritic effects. *Brain stimulation* 10, 51-58.
- 616 Laczo, B., Antal, A., Rothkegel, H., Paulus, W., 2014. Increasing human leg motor cortex excitability by
617 transcranial high frequency random noise stimulation. *Restor Neurol Neurosci* 32, 403-410.
- 618 Lafon, B., Rahman, A., Bikson, M., Parra, L.C., 2017. Direct current stimulation alters neuronal
619 input/output function. *Brain stimulation* 10, 36-45.
- 620 Lee, K.Y., Bae, C., Lee, D., Kagan, Z., Bradley, K., Chung, J.M., La, J.-H., 2020. Low-intensity, kilohertz
621 frequency spinal cord stimulation differently affects excitatory and inhibitory neurons in the rodent
622 superficial dorsal horn. *Neuroscience*.
- 623 Lempka, S.F., McIntyre, C.C., Kilgore, K.L., Machado, A.G., 2015. Computational analysis of kilohertz
624 frequency spinal cord stimulation for chronic pain management. *Anesthesiology: The Journal of the*
625 *American Society of Anesthesiologists* 122, 1362-1376.
- 626 Lesperance, L.S., Lankarany, M., Zhang, T.C., Esteller, R., Ratte, S., Prescott, S.A., 2018. Artfactual
627 hyperpolarization during extracellular electrical stimulation: Proposed mechanism of high-rate
628 neuromodulation disproved. *Brain stimulation* 11, 582-591.
- 629 Lessmann, V., Heumann, R., 1998. Modulation of unitary glutamatergic synapses by neurotrophin-4/5 or
630 brain-derived neurotrophic factor in hippocampal microcultures: presynaptic enhancement depends on
631 pre-established paired-pulse facilitation. *Neuroscience* 86, 399-413.
- 632 Litvak, L.M., Smith, Z.M., Delgutte, B., Eddington, D.K., 2003. Desynchronization of electrically evoked
633 auditory-nerve activity by high-frequency pulse trains of long duration. *J Acoust Soc Am* 114, 2066-2078.
- 634 McIntyre, C.C., Grill, W.M., 1999. Excitation of central nervous system neurons by nonuniform electric
635 fields. *Biophysical journal* 76, 878-888.
- 636 McIntyre, C.C., Grill, W.M., Sherman, D.L., Thakor, N.V., 2004. Cellular effects of deep brain stimulation:
637 model-based analysis of activation and inhibition. *J Neurophysiol* 91, 1457-1469.
- 638 Medeiros, F.V., Bottaro, M., Vieira, A., Lucas, T.P., Modesto, K.A., Bo, A.P.L., Cipriano Jr, G., Babault, N.,
639 Durigan, J.L.Q., 2017. Kilohertz and low-frequency electrical stimulation with the same pulse duration
640 have similar efficiency for inducing isometric knee extension torque and discomfort. *American journal of*
641 *physical medicine & rehabilitation* 96, 388-394.

- 642 Negahbani, E., Kasten, F.H., Herrmann, C.S., Fröhlich, F., 2018. Targeting alpha-band oscillations in a
643 cortical model with amplitude-modulated high-frequency transcranial electric stimulation. *Neuroimage*
644 173, 3-12.
- 645 Patel, Y.A., Butera, R.J., 2015. Differential fiber-specific block of nerve conduction in mammalian
646 peripheral nerves using kilohertz electrical stimulation. *Journal of neurophysiology* 113, 3923-3929.
- 647 Pelot, N., Grill, W., 2020. In vivo quantification of excitation and kilohertz frequency block of the rat
648 vagus nerve. *Journal of Neural Engineering* 17, 026005.
- 649 Pelot, N.A., Behrend, C., Grill, W., 2017. Modeling the response of small myelinated axons in a
650 compound nerve to kilohertz frequency signals. *Journal of Neural Engineering*.
- 651 Radman, T., Ramos, R.L., Brumberg, J.C., Bikson, M., 2009. Role of cortical cell type and morphology in
652 subthreshold and suprathreshold uniform electric field stimulation in vitro. *Brain stimulation* 2, 215-228.
653 e213.
- 654 Radman, T., Su, Y., An, J.H., Parra, L.C., Bikson, M., 2007. Spike timing amplifies the effect of electric
655 fields on neurons: implications for endogenous field effects. *Journal of Neuroscience* 27, 3030-3036.
- 656 Rahman, A., Lafon, B., Parra, L.C., Bikson, M., 2017. Direct current stimulation boosts synaptic gain and
657 cooperativity in vitro. *The Journal of physiology*.
- 658 Rahman, A., Reato, D., Arlotti, M., Gasca, F., Datta, A., Parra, L.C., Bikson, M., 2013. Cellular effects of
659 acute direct current stimulation: somatic and synaptic terminal effects. *The Journal of physiology* 591,
660 2563-2578.
- 661 Ranck, J.B., 1975. Which elements are excited in electrical stimulation of mammalian central nervous
662 system: a review. *Brain research* 98, 417-440.
- 663 Ranieri, F., Podda, M.V., Riccardi, E., Frisullo, G., Dileone, M., Profice, P., Pilato, F., Di Lazzaro, V., Grassi,
664 C., 2012. Modulation of LTP at rat hippocampal CA3-CA1 synapses by direct current stimulation. *Journal*
665 *of neurophysiology* 107, 1868-1880.
- 666 Reato, D., Rahman, A., Bikson, M., Parra, L.C., 2010. Low-intensity electrical stimulation affects network
667 dynamics by modulating population rate and spike timing. *Journal of Neuroscience* 30, 15067-15079.
- 668 Reato, D., Rahman, A., Bikson, M., Parra, L.C., 2013. Effects of weak transcranial alternating current
669 stimulation on brain activity—a review of known mechanisms from animal studies. *Frontiers in human*
670 *neuroscience* 7, 687.
- 671 Rubinstein, J.T., Wilson, B.S., Finley, C.C., Abbas, P.J., 1999. Pseudospontaneous activity: stochastic
672 independence of auditory nerve fibers with electrical stimulation. *Hear Res* 127, 108-118.
- 673 Shapiro, K., Guo, W., Armann, K., Pace, N., Shen, B., Wang, J., Beckel, J., de Groat, W., Tai, C., 2020.
674 Pudendal Nerve Block by Low-Frequency (≤ 1 kHz) Biphasic Electrical Stimulation. *Neuromodulation:*
675 *Technology at the Neural Interface*.
- 676 Terney, D., Chaieb, L., Moliadze, V., Antal, A., Paulus, W., 2008. Increasing human brain excitability by
677 transcranial high-frequency random noise stimulation. *J Neurosci* 28, 14147-14155.
- 678 Thomson, S.J., Tavakkolizadeh, M., Love-Jones, S., Patel, N.K., Gu, J.W., Bains, A., Doan, Q., Moffitt, M.,
679 2018. Effects of rate on analgesia in kilohertz frequency spinal cord stimulation: results of the PROCO
680 randomized controlled trial. *Neuromodulation: Technology at the Neural Interface* 21, 67-76.
- 681 Voroslakos, M., Takeuchi, Y., 2018. Direct effects of transcranial electric stimulation on brain circuits in
682 rats and humans. 9, 483.
- 683 Wang, B., Aberra, A.S., Grill, W.M., Peterchev, A.V., 2018. Modified cable equation incorporating
684 transverse polarization of neuronal membranes for accurate coupling of electric fields. *Journal of Neural*
685 *Engineering* 15, 026003.
- 686 Wang, Z., Pace, N., Cai, H., Shen, B., Wang, J., Roppolo, J.R., de Groat, W.C., Tai, C., 2020. Poststimulation
687 block of pudendal nerve conduction by high-frequency (kHz) biphasic stimulation in cats.
688 *Neuromodulation: Technology at the Neural Interface* 23, 747-753.

- 689 Ward, A.R., 2009. Electrical stimulation using kilohertz-frequency alternating current. *Physical therapy*
690 89, 181-190.
- 691 Zannou, A.L., Khadka, N., FallahRad, M., Truong, D.Q., Kopell, B.H., Bikson, M., 2019a. Tissue
692 Temperature Increases by a 10 kHz Spinal Cord Stimulation System: Phantom and Bioheat Model.
693 *Neuromodulation*.
- 694 Zannou, A.L., Khadka, N., Truong, D.Q., Zhang, T., Esteller, R., Hershey, B., Bikson, M., 2019b.
695 Temperature increases by kilohertz frequency spinal cord stimulation. *Brain stimulation* 12, 62-72.
- 696 Zhang, X., Roppolo, J.R., De Groat, W.C., Tai, C., 2006. Mechanism of nerve conduction block induced by
697 high-frequency biphasic electrical currents. *IEEE Transactions on Biomedical Engineering* 53, 2445-2454.
- 698 Zhao, S., Yang, G., Wang, J., Roppolo, J.R., de Groat, W.C., Tai, C., 2014. Effect of non-symmetric
699 waveform on conduction block induced by high-frequency (kHz) biphasic stimulation in unmyelinated
700 axon. *Journal of computational neuroscience* 37, 377-386.

701